William J. Todd*
Dale G. Gehring
Technicolor Graphic Services, Inc.
EROS Data Center
Sioux Falls, SD 57198
Jon F. Haman
National Park Service
Denver Service Center
Denver, CO 80225

Landsat Wildland Mapping Accuracy

Classification errors were attributable to the Landsat system itself, to project mapping objectives, and to analysts' decisions.

Abstract: *A Landsat-aided classification of ten wildland resource classes was developed for the Shivwits Plateau region of the Lake Mead National Recreation Area. Single stage cluster sampling (without replacement) was used to verify the accuracy of each class. For verification, 63 plots were randomly selected throughout the classification image (gridded into 52 ha cells), located on 1:30,000 scale black-and-white aerial photographs, and gridded into nine 5.8 ha cells each. Resource specialists interpreted the 5.8 ha cells, field checked selected sites from light aircraft, and re-checked their photointerpretation. Construction of contingency tables revealed that there was less confusion between aggregated (more generalized) resource classes—grouped on the basis of soils, terrain, and vegetative cover similarities—than detailed resource categories. Parametric calculations of percentages correct and confidence intervals fully supported those findings.*

Introduction

Digital image processing of Landsat data to derive land-cover classes was conducted by the EROS Data Center (EDC) and the National Park Service (NPS) to aid in resource management in the Lake Mead National Recreation Area (LMNRA). Resource map overlays and image products were compiled, and NPS personnel evaluated their utility and applications to the wide-ranging LMNRA planning effort. Details of one of the project's technical elements—accuracy assessment of a Landsat digital classification—form the basis for this article. Four distinct topical areas were involved:

- Generalized, large-area mapping of vegetation and terrain in an arid wildland environment. Two examples include Garvin and Pascucci (1973) and Tueller *et al.* (1975).
- Landsat MSS data characteristics (see Taranik (1978) for a concise overview).
- Digital image processing techniques (Bernstein and Ferneyhough, Jr. (1975) and Rohde (1978) are two general references), especially pattern recognition and discriminant analysis (see Swain, 1972).
- Quantitative accuracy assessment (Cochran, 1963).

The first three topics are well documented, but quantitative techniques are only occasionally used to assess the accuracy of Landsat digital classifications. Remote sensing literature is limited in describing map accuracy assessment procedures, and subsequently explaining the results by examining the first three items outlined

* Now with Technicolor Graphic Services, Inc., NASA-Ames Research Center, Moffett Field, CA 94035.

Photogrammetric Engineering and Remote Sensing,
Vol. 46, No. 4, April 1980, pp. 509-520.

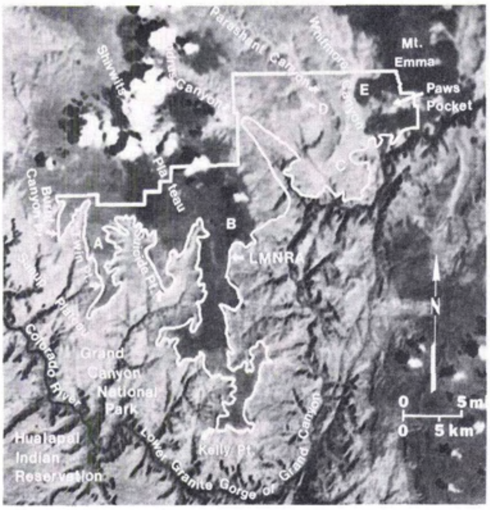

FIG. 1. Portion of Landsat Band 7 image (1303-17441-7) collected 22 May 1973 over Shivwits Plateau sector of Lake Mead National Recreation Area. Pinyon-Juniper woodland located at A and B; note higher reflectance of soils derived from limestone at A than soils derived from basalt at B. Shrub vegetation on soils derived from limestone (C) and steep talus slopes with an eastern exposure (D) have higher reflectance characteristics than the Pinyon-Juniper woodland (A, B) and basalt flows with sparse vegetative cover (E).

above. Using the 63,000 hectare Shivwits Plateau region (Figure 1, eastern portion of the LMNRA) as an example, we have attempted to fill this information gap.

METHODS

LANDSAT DATA PREPROCESSING AND CLASSIFICATION

The four-band Landsat digital data collected 22 May 1973 were subjected to standard preprocessing, clustering, and classification techniques using the ESL Interactive Digital Image Manipulation System (IDIMS) (Rohde, 1978). Preprocessing included histogram normalization, precision geometric correction, and spatial masking to exclude data outside the LMNRA boundary. Resampling of the data created 80 by 80 metre pixels geometrically registered to a UTM grid.

A clustering technique was used to derive resource classes for the Shivwits Plateau (Figure 2). First, an algorithm randomly located 15 by 15 pixel cluster sites throughout the area, whose combined area equaled 10 percent of the region's total area. The spatial distribution of the 49 selected cluster sites was superimposed onto a Landsat color composite and examined. Because all spectral variability within the region had not been accounted for, four sites were manually, electronically delineated using an interactive CRT device. All 53 cluster sites were submitted as a single data set to a clustering algorithm, which used the four Landsat bands to group the data into 39 clusters. Cluster means, variances, and covariance matrices were input to a Gaussian maximum likelihood classifier, which was used to classify three manually-chosen sites representative of terrain and vegetation within the Shivwits Plateau region. Visual evaluation of the classification results of these sites was good, and classification of the entire region was performed.

A preliminary grouping of the cluster classes into resource classes was modified after field checking, which indicated that certain cluster groupings were incorrect and that selected resource class descriptions were erroneous and/or incomplete. Field data were used to obtain the final cluster groupings (Figure 2c) and associated resource class descriptions (Table 1).

Another problem was the presence of ten small cumulus clouds and their shadows at the time of the Landsat overpass (Figure 1). Four spectral classes had been obtained for cloud shadow and three classes for cloud (not shown in Figure 2). High altitude aerial photographs were used to map the resource types obscurred by the clouds and shadows; the new data were digitally inserted into the classification file.

Spatial stratification was used to resolve classification problems with clusters 2, 6, and 32 (Figures 2b and 2c). Pixels classified into cluster 32 were interspersed within basalt flows as well as throughout the pinyon-juniper woodland on the Shivwits Plateau. Those pixels were divided spatially between (1) basalt flows, (2) sparse pinyon-juniper on basalt, and (3) sparse pinyon-juniper on limestone. Pixel changes (the two sparse pinyon-juniper classes became new resource classes) were executed by manually locating the appropriate terrain boundaries on an interactive CRT device and using an algorithm to "change" pixel classification within designated regions. Similarly, pixels of clusters 2 and 6—occurring principally within basalt flows—were incorrectly located within the pinyon-juniper woodland region. In that part of the plateau woodland developed on soils derived from basalt, those pixels of clusters 2 and 6 were added to the medium-density pinyon-juniper on basalt category. Within the limestone region, pixels of clusters 2 and 6 were added to the sparse pinyon-juniper on limestone.

A pixel of 0.64 hectares is a relatively

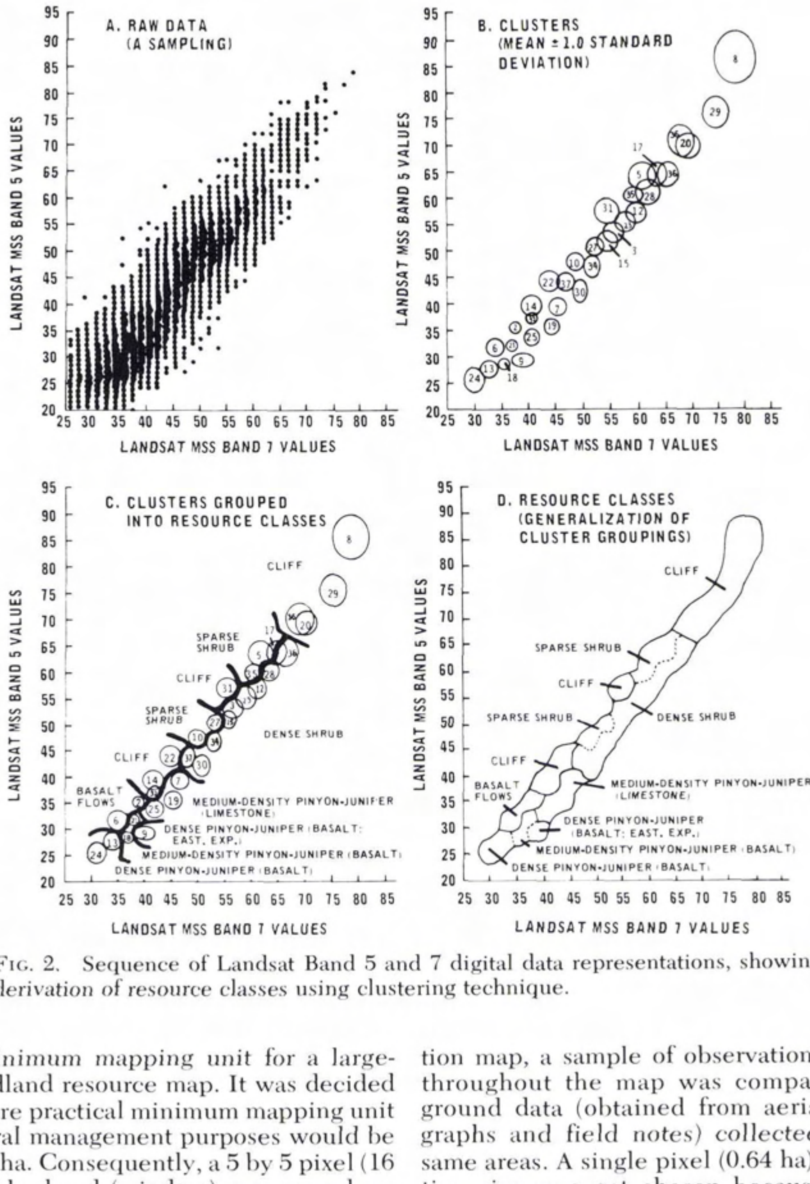

FIG. 2. Sequence of Landsat Band 5 and 7 digital data representations, showing derivation of resource classes using clustering technique.

small minimum mapping unit for a large-area wildland resource map. It was decided that a more practical minimum mapping unit for general management purposes would be about 16 ha. Consequently, a 5 by 5 pixel (16 ha) neighborhood (window) was moved sequentially through the image, smoothing the classification by changing the window's center pixel class designation to that which occurred most frequently within the window. Both smoothed and unsmoothed classification maps were ultimately requested by the NPS, the former showing generalized results and the latter revealing the (more realistic) complexities of vegetation/terrain patterns. Accuracy assessment was performed on the smoothed classification results.

ACCURACY ASSESSMENT

To estimate the accuracy of the classification map, a sample of observations located throughout the map was compared with ground data (obtained from aerial photographs and field notes) collected for the same areas. A single pixel (0.64 ha) observation size was not chosen because (1) the mean residual error of the geometric registration was about one pixel (a single pixel could not have been reliably located on an aerial photograph) and (2) the classification image had been spatially smoothed. Conversely, the 5 by 5 pixel (16 ha) sized observation—the size of the classification smoothing window—was deemed too large for verifying map accuracy. A 3 by 3 pixel (5.8 ha) observation was used as a compromise.

Single-stage cluster sampling (without replacement) was used to calculate the minimum number of observations needed to estimate the accuracy of each class. Using the formula

TABLE 1. RESOURCE CLASS DESCRIPTIONS FOR COMPUTER-ASSISTED, LANDSAT-DERIVED CLASSIFICATION OF LMNRA'S SHIVWITS PLATEAU REGION

Resource Class (short name)	Dominant plant types	Secondary species	Overstory crown closure	Vegetative Ground Cover	Primary Soil Parent Mat.	Other Characteristics
Dense pinyon-juniper on basalt	*Pinus monophylla* and *Juniperus osteosperma* (pinyon-juniper)	*Pinus ponderosa* (ponderosa pine) along drainage ways	>30% (and often >50%)		basalt	
Dense pinyon-juniper on basalt with eastern exposure	*Pinus monophylla* and *Juniperus osteosperma* (pinyon-juniper)	*Quercus gambelli* (gambel oak)	>20%		basalt	eastern exposure and >20% slope
Medium density pinyon-juniper on basalt	*Pinus monophylla* and *Juniperus osteosperma* (pinyon-juniper)	*Pinus ponderosa* (ponderosa pine) and *Quercus gambelli* (gambel oak)	10–30%		basalt	
Sparse pinyon-juniper on basalt	*Pinus monophylla* and *Juniperus osteosperma* (pinyon-juniper)		5–15%		basalt	
Medium-density pinyon-juniper on limestone	*Pinus monophylla* and *Juniperus osteosperma* (pinyon-juniper)		10–30%		limestone of Kaibab Formation	light-red to tan soils
Sparse pinyon-juniper on limestone	*Pinus monophylla* and *Juniperus osteosperma* (pinyon-juniper)	*Artemisia tridentata* (sagebrush)	5–15%		limestone of Kaibab Formation	light-red to tan soils
Sparse shrub	*Coleogyne ramosissima*, *Gutierrezia sarothrae*, *Larrea tridentata*, and *Yucca baccata*			<10%	limestone of Kaibab Formation	light-red to tan soils

Dense shrub	*Coleogyne ramosissima, Gutierrezia sarothrae, Larrea tridentata,* and *Yucca baccata*	*Jumiperus osteosperma* (juniper)	>10% (and often >75%)	limestone of Kaibab Formation	light-red to tan soils
Cliff and slopes (<60%)	*Artemisia tridentata* (sagebrush), *Juniperus osteosperma* (juniper)		<3%	limestone or sandstone	percent grade >60%
Basalt flows	*Larrea tridentata, Yucca baccata*		<5%	basalt	

$$n_i = \frac{N_i \hat{p}_i \hat{q}_i}{(N_i)(E^2/t^2) + \hat{p}_i \hat{q}_i},$$

where n_i is the sample size (number of observations) of class i,
N_i is (total size of class i) ÷ (9),
$\hat{p}_i$ is the estimated accuracy of class i (estimate provided by preliminary classification evaluation by NPS personnel),
E is the allowable error,
t is the Student's t statistic at the allowable error, and
$\hat{q}_i$ is $(1 - \hat{p}_i)$.

it was calculated that nearly 400 observations would need to be made (Table 2). Because project time and budget constraints prohibited such a large task, the observations were grouped into 9 by 9 pixel (51.8 ha) sample units (SU's), each SU containing nine 3 by 3 pixel observations. Hereafter, the following terminology is used:

- pixel: single Landsat data element (0.64 ha).
- observation: matrix of 3 by 3 pixels (5.8 ha).
- sample unit: matrix of 3 by 3 observations, or 9 by 9 pixels (51.8 ha).

The Landsat data were gridded into 51.8 ha sample units (SU) (Figure 3). A random sample of SU's were drawn and alphanumeric line printer classification maps were printed for each showing pixel class assignments (Figure 4). Each observation cell was checked for two conditions before the SU was selected for accuracy assessment: (1) at least five contiguous pixels of the nine in the cell must be of the same class, and (2) whether the observation was needed to satisfy the minimum number of required observations as computed in the simple random sampling equation. By satisfying the second requirement for the more sparsely distributed resource classes, more observations were obtained for other classes than were required (Table 2). It was decided that all 510 eligible observations of the 63 selected SU's would be used for accuracy assessment because (1) it would take relatively little additional time to collect ground data for the other observations located within the SU, and (2) variances of the accuracy estimates might be reduced by including extra observations.

To locate SU's on aerial photographs, the geometric control network was referenced to calculate longitude and latitude coordinates of SU corners. Locations were plotted on Arizona 1:24,000 orthophotoquad map

TABLE 2. SINGLE-STAGE CLUSTER SAMPLING PARAMETERS

Resource class	N_i[1]	$\hat{P}_i$[2]	E[3]	n_i[4]	L[5]
Dense pinyon-juniper on basalt with eastern exposure	227	0.80	0.10	36	36
Dense pinyon-juniper on basalt	372	0.80	0.10	39	37
Medium density pinyon-juniper on basalt	2562	0.80	0.10	43	116
Sparse pinyon-juniper on basalt	93	0.80	0.10	30	29
Medium density pinyon-juniper on limestone	1685	0.80	0.10	42	74
Sparse pinyon-juniper on limestone	25	0.80	0.10	16	11
Dense shrub	1454	0.70	0.10	55	60
Sparse shrub	3213	0.70	0.10	56	92
Basalt flows	554	0.90	0.10	23	24
Cliff & slopes (>60%)	674	0.85	0.10	33	31

[1] (Total number of resource class pixels) ÷ 9.
[2] Estimated accuracy of resource class.
[3] Allowable error.
[4] Required sample size (number of 3 by 3 pixel observations) for resource class, as computed from single-stage cluster sampling equation.
[5] Number of observations selected for accuracy assessment.

sheets (where available) or on USGS 1:24,000 scale topographic quadrangles, and subsequently transferred to NPS 1:30,000 scale black-and-white aerial photographs taken in 1970 (Figure 4). Each SU photo plot was checked for locational accuracy by examination of the gridded Landsat color composite image. The majority of SU locations were spatially adjusted.

For each sample unit, an accuracy assessment worksheet was prepared that showed where class boundaries occurred within observations. Only that portion of an observation having at least five contiguous pixels of

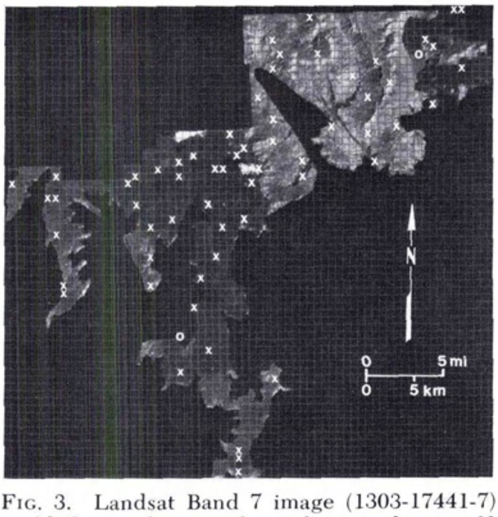

FIG. 3. Landsat Band 7 image (1303-17441-7) gridded into 9 by 9 pixel sample units showing 63 randomly-selected samples for accuracy assessment. The two samples indicated by zeros are shown in Figure 4.

the same class was subject to ground data acquisition (Figure 4).

Annotated worksheets and aerial photographs (with plotted SU overlays) were submitted to a team of project participants who were not intimately knowledgeable with the final classification results and who could, therefore, collect unbiased ground data. This team was also provided with a list of the preliminary resource class definitions from which it devised a classification key.

The initial step in placing each observation into one of the ten resource categories was to determine if the sample was located within the light red or tan soils developed on the Kaibab Formation, or within basalt and basaltic soils. This distinction was accomplished by checking the SU location on a 1:250,000 scale photo mosaic on which the principal soils boundaries were plotted. After assigning samples to a soils category, photo interpretation techniques were used to go through the remaining steps of the key. Each of the 510 observations was assigned to a resource class, based upon the spatially dominant class.

While the photo interpretation was being done, careful notes were made directly onto the worksheets whenever interpretation or definitional difficulties arose. The aerial photographs and completed worksheets were taken to the LMNRA, where observations from an airplane were used to field check selected samples. Most of the difficulties which occurred during the interpretation had been related to vegetative cover density, both woodland crown closures within the upland plateau areas and shrub densities at lower elevations. Field notes were taken, as

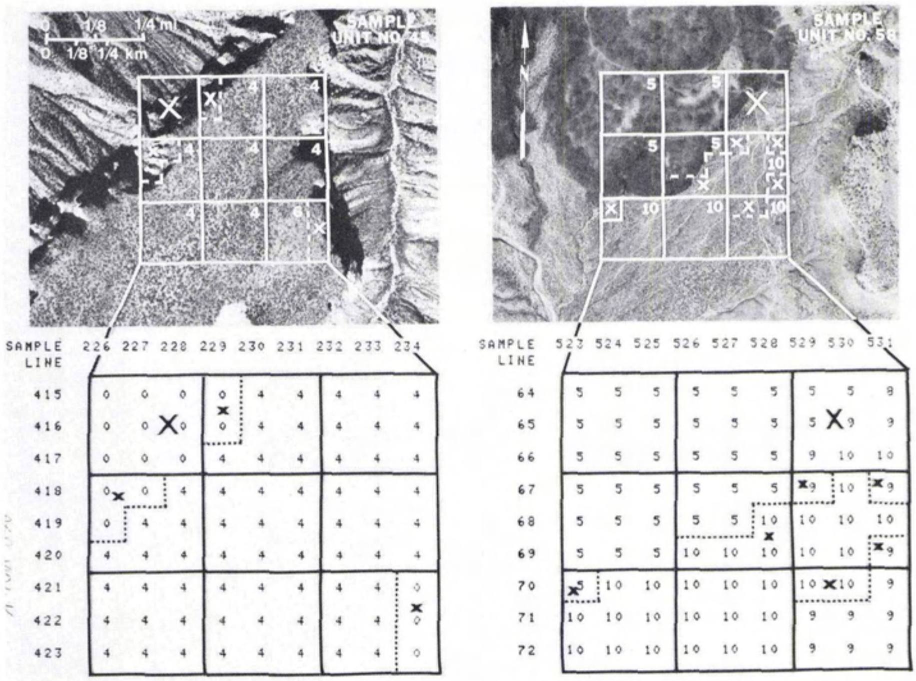

FIG. 4. Aerial photographs (upper) and computer-assisted, lineprinter classification maps of Landsat data (lower) of two example sample units, each gridded into nine 3 by 3 pixel observations. Resource classes: 0—data outside LMNRA boundary; 4-medium-density pinyon-juniper on soils derived from basalt; 6—sparse pinyon-juniper on soils derived from basalt; 5—basalt flows with sparse vegetative cover; 8—cliffs and talus slopes with >60% slope; 9—sparse shrub association; 10—dense shrub association. Observation portions indicated by X not photointerpreted. Note that lower-right observation of each sample contains an incorrect Landsat observation, according to the photointerpretation.

well as oblique photos of certain sites for further documentation.

All interpretations were methodically reexamined to insure that they were consistent, that is, that interpretation criteria had been applied in the same fashion to all 510 observations.

After completing the photo interpretation, the corresponding line printer maps of the machine-aided classification results were compared with the recorded ground data. Two of the classes—Dense Pinyon-Juniper on Basalt (Eastern Exposure) and Cliffs—had very few ground data observations. It was reasoned that the problem stemmed from incorrect or incomplete definitions of the classes, which caused assignment to other resource classes. For both of these classes a percentage slope element was added to the definition. The Dense Pinyon-Juniper on Basalt (Eastern Exposure) category was modified by adding the term ">20 percent Grade," while the Cliffs category was changed by adding the element ">60 percent Grade." The effect of each addition was to broaden the category definition. Aerial photographs, worksheets, and the revised definitions were returned to the project team that had acquired the ground data. They used a percent grade template to measure slope of all 510 observations plotted on USGS 1:24,000 scale topographic quadrangle maps. Revised interpretations were recorded on the original worksheets.

RESULTS

Two types of cross-tabulations and comparisons were made between the Landsat-derived and ground data sets: (1) creation of contingency tables, or confusion matrices, and (2) calculation of percentage correct for each class, including statistical confidence interval.

To prepare the contingency table (Table 3), each observation was checked to determine both the ground data categorization and the Landsat-aided classification. Such a table is useful because it shows which re-

TABLE 3. RESOURCE CLASS CONTINGENCY TABLE (10-CLASS)

# Ground observations: Resource class	# Landsat observations: Dns. pi-ju bas. east exp.	Dns. pi-ju bas.	Med pi-ju bas.	Sprse pi-ju bas.	Med. pi-ju lmst.	Sprse pi-ju lmst.	Dense shrb	Sprse shrb	Bas. flows	Cliffs	Total
Dns. pin.-jun. (bas.; east exp.)	4		3		1						8
Dns. pin.-jun. (bas.)	9	7	13								29
Med. dns. pin.-jun. (bas.)	17	27	86	27	5						162
Sprse pin.-jun. (bas.)	4	3	13	2							22
Med. dns. pin.-jun. (lmstne.)	2		1		62	7		11			83
Sprse pin.-jun. (lmstne.)					5		12	19		1	37
Dense shrub							40	53	4	9	106
Sparse shrub					1	4	7	7	1	7	27
Basalt flows									18	1	19
Cliffs & slopes (>60%)							1	2	1	13	17
Total	36	37	116	29	74	11	60	92	24	31	510

source classes are confused with each other, based upon the sample. Most of the confusion between classes occurred within groups of resource classes with similar ground cover composition. For example, the four Pinyon-Juniper (Basalt) classes were more often confused with each other, rather than with the other six resource classes. Utilizing this natural hierarchy within the classification—based upon terrain, soils, and vegetative similarities—the data from Table 3 were aggregated to reveal the more general relationships within the Landsat-aided classification (Table 4).

The contingency tables represent a nonparametric, descriptive mode of reporting the accuracy assessment data, while calculation of percentages correct and confidence intervals gives the resource manager a parametric estimate of the reliability of the accuracy estimates. Percentage correct is calculated for each class by the equation

$$C_j = \frac{\sum_{k=1}^{n} b_{jk}}{\sum_{k=1}^{n} a_{jk}} (100)$$

where C_j is the percent correct for class j,
b_{jk} is the number of observations correctly classified into class j in sample k, and
a_{jk} is the number of observations of class j in sample k, as determined from ground data

To calculate confidence intervals, the standard error of the estimate C_j must be found by the equation

$$E(C_j) = \left(\frac{\sqrt{1-h}}{\sqrt{n}\,\bar{a}_j} \right) \cdot \sqrt{\frac{\sum_{k=1}^{n} \left[b_{jk} - \left(\frac{C_j}{100} \right) \; (a_{jk}) \right]^2}{n-1}} (100)$$

where $E(C_j)$ is the standard error of estimate of C_j,
C_j is the percent correct for class j,
n is the number of samples units for class j,

TABLE 4. RESOURCE CLASS CONTINGENCY TABLE (5-CLASS)

	Generalized resource class	# Landsat observations					
		Pi-ju bas	Pi-ju lmstne	Shrub	Bas	Cliff & slopes	Total
# Ground observations	Pinyon-juniper (basalt)	215	6				221
	Pinyon-juniper (limestone)	3	74	42		1	120
	Shrub		5	107	5	16	133
	Basalt				18	1	19
	Cliff & slopes (>60%)			3	1	13	17
	Total	218	85	152	24	31	510

$\bar{a}_j$ $\sum_{k=1}^{n} a_{jk} \div n$,
h is $n \div N$ (N is total number of sample units in project area),
a_{jk} is the number of observations of class j in sample k, as determined from ground data, and
b_{jk} is the number observations correctly classified into class j in sample k.

Finally, statistical confidence intervals are calculated using the equation

$$I_j = C_j \pm [t]\,[E(C_j)]$$

where I_j is the confidence interval for class j,
C_j is the percent correct for class j,
t is the appropriate critical value of Student's t distribution, and
$E(C_j)$ is standard error of the estimate of C_j.

The "t" statistic used in the above formula was the appropriate value for each class at the 0.10 level of significance (90 percent probability level). Percent correct and confidence interval for each class are listed in Table 5.

DISCUSSION

Results of the accuracy assessment may be explored by examination of three elements: (1) the Landsat system, (2) project mapping objectives, and (3) analysts' decisions.

LANDSAT SYSTEM

Landsat data preprocessing included histogram normalization and geometric registration of the data to a desired map projection. Both processes resulted in an improved data set, but also had residual errors which probably had negative effects on the accuracy results.

Histogram normalization (destriping) resulted in a data set which did have residual

TABLE 5. ACCURACY ASSESSMENT AND AREA CALCULATIONS

Resource Class	Accuracy Assessment		Area Calculations	
	Stand. Error of Est. (%)	% Correct & Conf. Int.	# Hectares	% Total Area
Pinyon-Juniper (Basalt)	0.6	97.3 ± 1.4	18,719	29.9
Dense, East. Exp.	14.2	50.0 ± 78.9	1,302	2.1
Dense	12.5	24.1 ± 26.4	2,139	3.4
Medium Density	2.9	53.1 ± 5.0	14,742	23.6
Sparse	9.4	9.1 ± 18.3	536	0.9
Pinyon-Juniper (Limestone)	11.0	61.7 ± 19.2	9,842	15.7
Medium density	7.4	74.7 ± 13.2	9,699	15.5
Sparse	—	0	143	0.2
Shrub Associations	6.4	80.5 ± 11.0	26,969	43.1
Dense	8.2	37.7 ± 14.4	8,480	13.5
Sparse	9.2	25.9 ± 16.9	18,489	29.5
Basalt Flows	4.9	94.7 ± 14.3	3,188	5.1
Cliffs & Slopes (>60%)	18.4	76.5 ± 39.2	3,879	6.2

striping. The striping was more visually evident in the raw Landsat images than in the maximum likelihood classification image. Although visual evidence of striping was completely removed after smoothing the classification image, the initial effect of the radiometric defect probably caused classification error.

Geometric registration errors were about one pixel, as tested on the control point network used to develop the geometric transformation. Registration errors were noticed when checking the airphoto plots of the sample units (as originally determined from the control point network) against a gridded Landsat color composite. Image interpretation was used to correct sample unit locations, but analyst errors were certainly made at that time also. Of course, the fact that the observation unit was five to nine pixels in size masked most of the geometric registration error.

PROJECT MAPPING OBJECTIVES

Detailed resource classes were sought for the Shivwits Plateau region. Reexamining Figure 2a, note that the dynamic range of the original data is relatively small, and that the clusters (Figure 2b) represent a large number of spectrally similar classes which correspond to the maximum raw data frequency concentration. Despite the fact that only two of the four Landsat bands are shown, the overlapping nature of the clusters—visually under-emphasized because only one standard deviation from the mean was drawn—indicates that derived resource class (Figures 2c and 2d) will be similar.

Not unexpectedly, there is a close association between spectral separability and the accuracy assessment results (Figure 5). Two resource classes containing cluster pairs with relatively low weighted divergence tended to be confused with each other, according to the ground data versus Landsat data comparison.

Justification for spatial, environmental stratification applied to the classification image—involving clusters 2, 6, and 32—is also revealed in Figure 5. [For the sake of diagrammatic clarity, we have indicated only the primary clusters of resource classes to

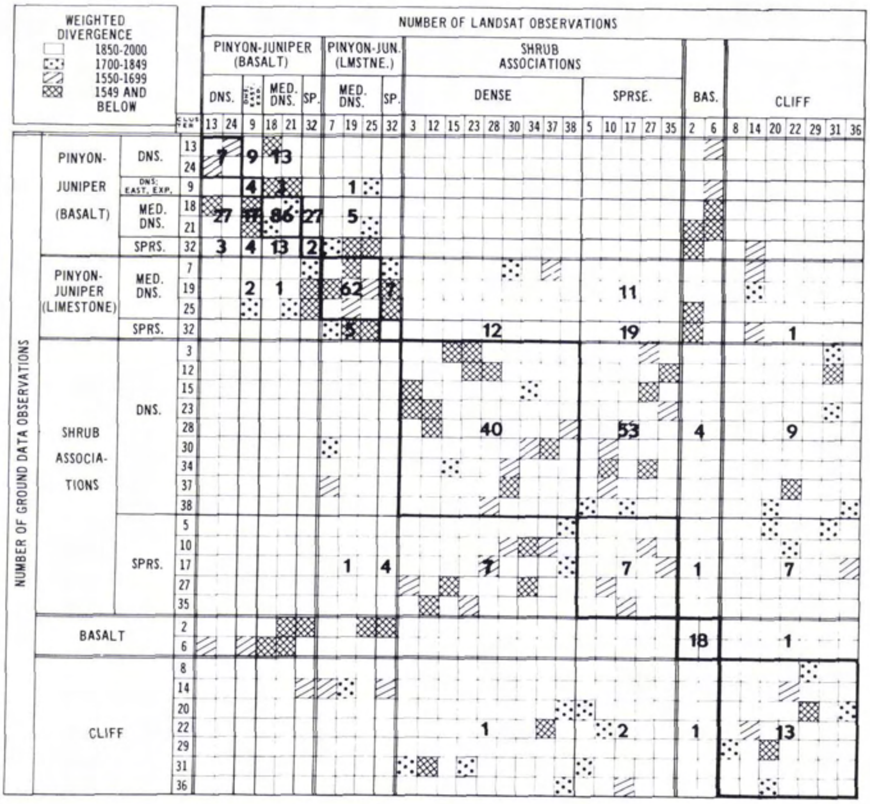

FIG. 5. Comparison of resource class contingency table with weighted divergence between cluster class pairs.

which stratification was applied. Clusters 2 and 6 were also a part of Medium Density Pinyon—Juniper (Basalt) and Sparse Pinyon-Juniper (Limestone), and cluster 32 was part of Basalt Flows.] Nearly every cluster of Pinyon-Juniper (Basalt), for example, has relatively low spectral separability with one of the two Basalt Flow clusters; stratification was needed to separate these two spectrally similar resource classes.

ANALYSTS' DECISIONS

The problems of quantitative similarity of classes is compounded by at least three more considerations:

- The Landsat data are continuous (Figure 2a), alluding to the transitional situation of changing from one wildland resource class to another. There are no distinct, isolated resource classes in the Shivwits Plateau area, nor are there discrete spectral groupings in the satellite multispectral data.
- We may assume that there exist "correct" (optimum, best) boundaries within the Landsat four-vector space between desired resource classes. Using the clustering technique, however, we only obtained an approximation of those boundaries.
- The analysts must, in the end, define the resource class by describing the ground cover.

It is difficult, indeed, to describe the Landsat-derived resource classes, taking into account all of the above factors. Our final definitions (Table 1) do represent an attempt to consider the overlapping, transitional nature of the cluster resource classes and the approximation aspect of the clustering technique by using overlapping elements related to vegetative ground coverage. Within the upland forested categories we used overlapping crown closure percentages of the overstory, while within the shrub associations we used overlapping percentages of vegetative cover. Preliminary definitions had not included these overlap elements.

COSTS

The estimated $30,800 expended on the Shivwits Plateau portion of the LMNRA project included NPS and EDC costs associated with:

- Personnel— 48 percent
- Travel—18 percent
- Imagery, CCT's, supplies—10 percent
- Machine time—24 percent

Costs (Table 6) reflect the demonstration and training aspects of the LMNRA cooperative effort, and would be considerably lower in an operational mode. Personnel costs were high—some 12 NPS and EDC scientists were directly involved throughout most parts of the project. Of course, the high personnel costs resulted in higher administrative costs as well as travel expenditures (NPS sent three to five scientists to the EROS Data Center for several training and analysis workshops). Detailed procedural documentation (15 percent of costs) need not be as extensive in an operational project.

CONCLUSIONS AND RECOMMENDATIONS

We alluded above to three principal categories of classification error. The first category, Landsat system—geometric and radiometric problems related to preprocessing—probably accounts for only a small amount (perhaps 5 to 15 percent) of the error. Geometric and radiometric residual error are measurable, but we are aware of few studies which specifically discuss the effect of these errors on accuracy assessment results, both percentage correct and measures of variance or precision. More research is needed in this area.

The second category, project mapping objectives, refers to the detail of the resource classification scheme. We think that at least a third (perhaps 35 to 45 percent) of the classification error is directly related to trying to extract Landsat-derived resource classes whose spectral characteristics approach—and sometimes reach—the noise level of the data. Quantitative measures of separability (weighted divergence between cluster class pairs) were available, but the concept becomes very complex in consideration of large numbers of clusters and its subset of resource classes. Some research has been done in relating divergence to percentage correct (Swain and King, 1973), and we referred to the subject in a non-empirical

TABLE 6. ESTIMATED COSTS BY MAJOR TASKS FOR SHIVWITS PLATEAU ANALYSIS

Major Task	Estimated Cost	% of Subtotal
Planning	$ 1,600	7
Preprocessing	1,200	5
Classification	1,700	8
Post Classification	1,300	6
Accuracy Assessment	3,100	14
Field Work	3,000	14
Documentation	3,400	15
Administration	6,700	30
Subtotal	22,000	
Overhead (40%)	8,800	
TOTAL	$30,800	

fashion (Figure 5), but further investigations are needed.

The third and final category, analysts' decisions, we believe to have contributed about half (perhaps 45 to 55 percent) of the classification error. Each of the ten Landsat-derived resource classes appeared to represent a meaningful spatial pattern within the Shivwits Plateau region. Description of class polygons, however, required consideration of complex interaction between both vegetative and terrain characteristics of the arid wildland environment. Landscape definition is a scientific—yet subjective—process.

Acknowledgments

The authors thank Donald T. Lauer, U.S. Geological Survey, EROS Data Center, and Maurice Nyquist and Kenneth Raithel, National Park Service, Denver Service Center, for their support and guidance throughout the Lake Mead National Recreation Area Project. The work was done under U.S. Geological Survey Contract No. 14-08-0001-16439.

References

Bernstein, Ralph, and D. G. Ferneyhough, Jr., 1975. Digital Image Processing, *Photogrammetric Engineering and Remote Sensing*, Vol. 41, pp. 1465-1476.

Cochran, William G., 1963. *Sampling Techniques*, 2nd Ed., John Wiley & Sons, Inc., New York, NY, 413 pp.

Garvin, Lester E., and Richard F. Pascucci, 1973. Remote Sensing and Analysis of Soils and Vegetation Resources in the California Desert, in *Proceedings of the Fourth Annual Conference on Remote Sensing in Arid Lands*, Tucson, Arizona, University of Arizona, pp. 359-374.

Rohde, Wayne G., 1978. Digital Image Analysis Techniques Required for Natural Resource Inventories, in *Proceedings of the National Computer Conference*, AFIPS Press, Montvale, NJ, pp. 93-106.

Swain, Philip H., 1972. *Pattern Recognition: A Basis for Remote Sensing Data Analysis*, LARS Information Note 111572, Purdue University, W. Lafayette, IN, 40 pp.

Swain, P. H., and R. C. King, 1973. Two Effective Feature Selection Criteria for Multispectral Remote Sensing, in *Proceedings of the First International Joint Conference on Pattern Recognition*, Washington, DC, IEEE Catalog No. 73 CHO 821-9C, pp. 536-540.

Taranik, James V., 1978. *Characteristics of the Landsat Multispectral Data System*, U.S. Geological Survey Open-File Report 78-187, EROS Data Center, Sioux Falls, SD, 76 pp.

Tueller, Paul T., Garwin Lorain, Ron Halvorson, and Joe M. Ratliff, 1975. Mapping Vegetation in the Great Basin from ERTS-1 Imagery, in *Proceedings of the 41st Annual Meeting of the American Society of Photogrammetry*, American Society of Photogrammetry, Falls Church, VA, pp. 338-370.

(Received 2 April 1979; revised and accepted 10 October 1979)

Short Courses

The Application of Remote Sensing Techniques to Environmental Resource Problems

Terre Haute, Indiana
16–20 June 1980
18–22 August 1980

These five-day short courses, developed by the Indiana State University Remote Sensing Laboratory (ISURSL) and the Laboratory for the Application of Remote Sensing (LARS) at Purdue University, will focus on applied remote sensing, with emphasis on machine-assisted processing of multispectral data and visual interpretation of aerial photography and electronically synthesized images for environmental resource evaluation and planning. Participants will study (1) the potential of remote sensing; (2) principles of remote sensing, including various types of machine-assisted processing techniques; (3) types, sources, and uses of remote sensing products; and (4) specific environmental resource applications which have been conducted by LARS and ISURSL.

For further information abut the program, please contact

Dr. Paul W. Mausel, Director, ISURSL
Department of Geography & Geology
Indiana State University
Terre Haute, IN 47809
Telephone (812) 232-6311, ext. 2444